Acta Derm Venereol (Stockh) 1993; 73: 323–329

Quantitative and 3-Dimensional Analysis of Langerhans' Cells Following Occlusion with Patch Tests Using Confocal Laser Scanning Microscopy

AXEL EMILSON[1,3], MAGNUS LINDBERG[2,3], BO FORSLIND[3] and ANNIKA SCHEYNIUS[1]

[1] *Department of Clinical Immunology, Karolinska Hospital, Stockholm,* [2] *Department of Dermatology, University Hospital, Uppsala and* [3] *Experimental Dermatological Research Group, Department of Medical Biophysics, Karolinska Institute, Stockholm, Sweden*

Quantitative and detailed 3-dimensional (3-D) morphological information can be obtained from the same tissue volume using a confocal laser scanning microscope (CLSM). In the present study, we used CLSM for evaluation of Langerhans' cells (LC) in human skin at 0 h, 24 h and 48 h following occlusion with patch tests for 48 h. The relative volume of epidermal CD1a reactivity was quantified with CLSM on 25 µm thick sections stained with indirect immunofluorescence. No statistically significant difference was found when comparing the values obtained on the biopsy specimens from occluded skin ($n = 36$) with those from non-occluded skin ($n = 9$). Nor were any statistically significant changes detected in the number of epidermal CD1a+ cells as determined with immunoperoxidase staining between occluded and non-occluded skin. The occlusion produced a transient mild inflammatory reaction with an induced expression of intercellular adhesion molecule-1 (ICAM-1) on keratinocytes and an increased number of CD3+ epidermal lymphocytes. In addition, 3-D reconstructions revealed spatial information on the distribution of LC dendrites towards the skin surface. ***Key words: Human skin; Stereology; Immunohistochemistry; Comparative study.***

(Accepted March 29, 1993.)

Acta Derm Venereol (Stockh) 1993; 73: 323–329.

A. Emilson, Department of Clinical Immunology, Karolinska Hospital, S-104 01, Stockholm, Sweden.

Occlusive patch tests are extensively used in the assessment of contact allergy, and a number of various test systems are available at present. Occlusion of the skin is also used in transdermal drug-delivery systems (1). It induces changes in the skin physiology and the barrier capacity of stratum corneum. Several effects have been described, such as increased mitotic activity in epidermis (2), increased hydration of stratum corneum (1) and increased wound healing (1, 3, 4). Following occlusion with patch tests, alterations in the Langerhans' cell (LC) population have been described at the ultrastructural level, including abnormally large vacuoles, dilated rough endoplasmatic reticulum and more villous cell membranes (5–7). Occlusion will also induce time-dependent variation in the volume of the intercellular space (5).

Conflicting data exist concerning the effect of occlusion on the number of LC in epidermis. Occlusion with Finn chamber® with water for 48 h has been reported to induce a tendency of a reduced number of LC in epidermis 24 h after the occlusion (7). In contrast, occlusion with Finn chamber® with water for 24 h has been demonstrated to increase the number of epidermal LC at 72 h following the occlusion (8). On the other hand, occlusion with empty silver-patch tests for 6 h, 1, 2, 4 and 7 days showed no differences in the number of LC compared to non-occluded skin (9).

The differences found in literature on the effects of occlusion on the number of LC in epidermis might be related to the methods used (10). When estimating alterations in cell numbers and in expression of surface markers, ordinary light microscopy is not sufficient for making a complete description of qualitative and quantitative changes in one and the same tissue volume. This problem can be solved, however, with confocal laser scanning microscopy (CLSM). This technique has the following advantages compared to ordinary light microscopy: 1) increased resolution in the lateral (11) as well as in the vertical dimension (12); 2) elimination of out-of-focus light, thus enhancing contrast (13); 3) possibilities for horizontal optical and vertical optical sectioning (13); 4) 3-dimensional (3-D) reconstructions of the object (12, 14, 15); and finally 5) objective quantitative measurements on data using image analysis systems (13, 16).

In the present study we used CLSM to evaluate the effects on LC in human skin at 0 h, 24 h and 48 h after occlusion with epicutaneous patch tests for 48 h.

MATERIALS AND METHODS

Subjects

Nine healthy volunteers (age 24–40 years) with no clinical or anamnestic signs of skin diseases or atopy participated in the study. The study was approved by the Ethics Committee of the Karolinska Institute, Stockholm, and all volunteers gave their informed consent.

Occlusion

On each of the 9 volunteers the following four different types of occlusion were applied for 48 h: 1) True test® (Pharmacia, Uppsala, Sweden) without allergen; 2) empty Finn chamber® (diameter 8 mm); 3) Finn chamber® with distilled water (15 µl) on filter paper; and 4) Finn chamber® with petrolatum (approximately 15 µl). Non-occluded skin served as a control. The gluteal area was used to ascertain non sun-exposed skin.

The experiments were divided into three groups with 3 persons in each group. In group 1 (1 male, 2 females, age 30 years) the skin biopsy specimens were taken when the patch tests were removed after 48 h occlusion (0 h). In group 2 (3 males, age 26–40 years) the biopsies were taken 24 h after the occlusion, and in group 3 (3 males, age 24–26 years) they were taken 48 h after the occlusion.

The skin response to occlusion was graded visually at the time of biopsy, using a scale from 0 to +++, where 0 means no reaction, + = erythema, ++ = erythema with oedema and +++ = erythema, oedema and vesiculation.

Skin biopsy specimens

Punch biopsies (3 mm) were taken after intradermal injection of local anaesthesia (Lidocaine®, Astra, Sweden) from the four occluded skin

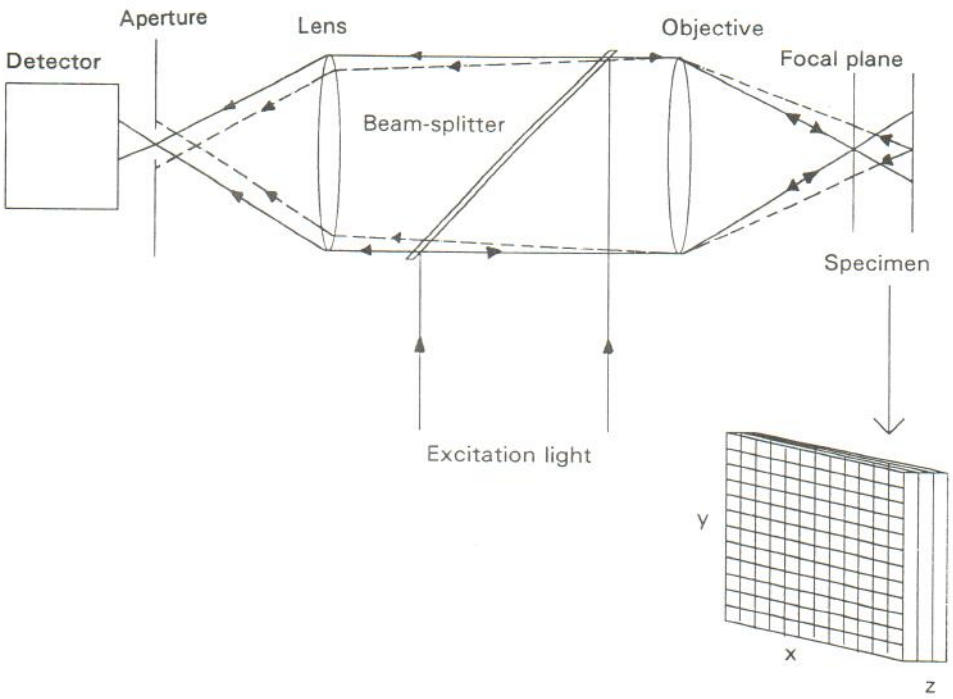

Fig. 1. The principle of CLSM. Each x, y, z position in the specimen is recorded as a picture element (pixel). Each pixel is assigned an intensity value depending on the strength of the emitted light.

sites and from non-occluded skin in each participant. The biopsies were immediately placed in transport medium (Histocon®, Histolab, Sweden) on ice and subsequently snap-frozen in chilled isopentane and stored at −70°C.

Indirect immunofluorescence staining for CLSM

Vertical cryostat sections, 25 μm thick, were fixed at +4°C in 50% (v/w) acetone for 30 s following 5 min in 100% acetone and were thereafter allowed to dry for 5 min at 22°C (room temperature). The sections were washed in phosphate-buffered saline (PBS) for 3×5 min and incubated with the mouse monoclonal antibody (MoAb) Leu-6 (IgG_{2bk}, cluster of differentiation: CD1a, Becton Dickinson, Sunnyvale, CA, USA) diluted 1/32, for 30 min at room temperature in a humidity chamber. After new washes in PBS for 3×5 min, the sections were allowed to react with the secondary antibody, fluorescein-isothiocyanate (FITC) labelled rabbit anti-mouse IgG, diluted 1/20, from Dakopatts, Copenhagen, Denmark, for another 30 min at room temperature. The sections were finally washed in PBS before they were mounted with glycerol in PBS containing p-phenylenediamine to reduce the fading of immunofluorescence during microscopy (17). Controls without the primary antibody gave no staining.

Confocal laser scanning microscopy

Comprehensive descriptions of the principle of CLSM have recently been published (13, 18). The following brief description is related to the SARASTRO® 2000 CLSM system (Molecular Dynamics, Sunnyvale, CA, USA). This beam-scanning system uses a Nikon Optiphot II microscope and an argon ion laser. The laser supplies three different excitation wavelengths: 457, 488 and 514 nm. The software for scanning and image processing was implemented on a Silicon Graphics 4D/25 personal Iris workstation, which is a UNIX-based system.

The principle of CLSM is point illumination and detection. A focused laser beam is used to scan the specimen. The secondary emission light from each illuminated spot is detected and stored as a digitized value (0–255) depending on the intensity of the light. Only light from the illuminated point is registered due to the small aperture placed in front of the detector (Fig. 1). Hence, the information obtained is almost free of out-of-focus light, giving a sharp picture of the focal plane. In the beam-scanning type of CLSM, scanning in x- and y-dimensions is usually managed by moving mirrors which position the laser beam towards every spot in the field of view. Scanning in the z-dimension is managed by a stepping motor, which refocuses the microscope to each focal plane. 3-D reconstructions of specimens can be obtained if a stack of consecutive optical sections is produced. Projections through the stack from different directions will produce views of the specimen volume, seen from different angles.

The 488 nm line was used for excitation of FITC. Detection of FITC was achieved with a beam-splitter reflecting at 510 nm, a confocal aperture diameter of 50 μm and, in front of the detector, a long-pass filter (510 nm).

Stereological measurements with CLSM

The examination was performed under coded conditions by one investigator (AE). Two sections from each biopsy specimen from one individual were stained and investigated on the same day. The presence of CD1a in epidermis was quantified using the following procedure. On each of the skin sections, the second and fifth fields of view from the left side of the skin section were chosen. In each field a stack of five optical sections was scanned, thus giving a total of twenty optical sections per skin biopsy. The optical sections in each stack were scanned with a z-increment of 3.0 μm, starting 5.0 μm from the top surface of the skin section. In order to determine the z-coordinate of the top surface, a vertical scan was performed on each skin section. The start position for the horizontal scanning of optical sections was given by this vertical scan.

From each optical stack an extended focus projection was calculated. An extended focus projection (Fig. 2A, D) is a 2-dimensional representation of 3-dimensional data. Each optical section is added to another, producing the extended focus projection where all optical sections are in focus. By using extended focus projections, the border of the basal layer of epidermis was well visualized giving a suitable map of epidermis. The pixel-data were processed using a threshold level algorithm (19). The intensity of all pixels in the picture is expressed as a logarithmic histogram. In this histogram a bend region indicates the separation of signal from noise. The threshold was set at the upper limit of the bend region. The same threshold, 40, was used for all optical sections. Binary pictures of each of the sections in each stack were produced, i.e. all pixels over the threshold were set to 1 (pix_1) and all pixels under the threshold were set to 0.

Each stack of binary pictures was evaluated using an image analysis system (ISIS, the Royal Institute of Technology, Stockholm, Sweden). A map of epidermis, excluding stratum corneum, was drawn for each extended focus projection (one for each stack of five optical sections). Repeated mapping by the same user showed the map area variation to

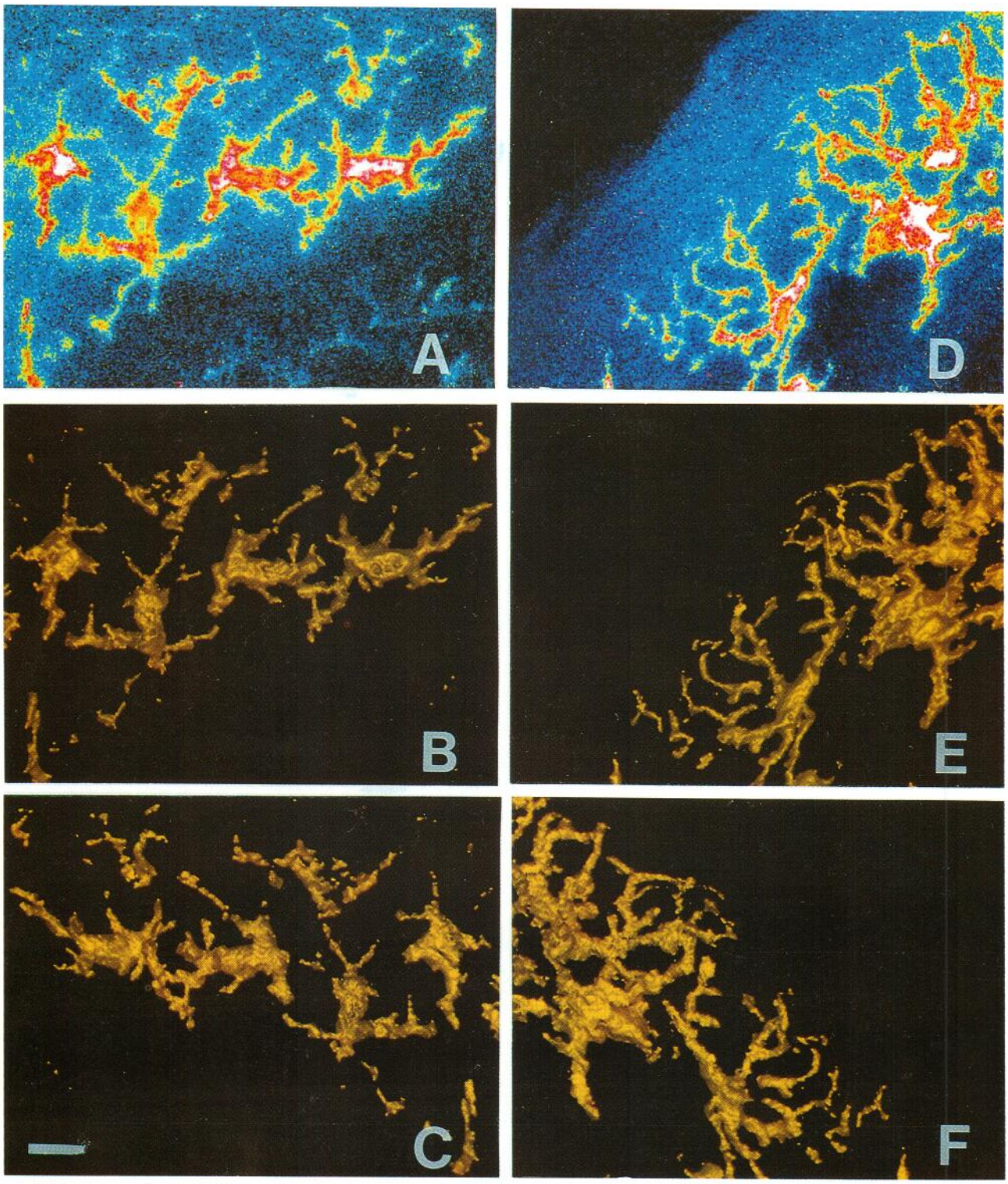

Fig. 2. 3-D reconstructions of LC from individual no. 3 in group 2. A biopsy from normal non-occluded skin (A–C) and a biopsy from skin occluded for 48 h with Finn chamber® and water (D–F) and biopsied 24 h later were analysed with CLSM. A ×100 plano-apochromate Nikon objective with oil-immersion was used. The pixel size was 0.2 μm × 0.2 μm and the picture size was 512 × 512 pixels. Optical stacks of 53 and 50 sections were scanned with a z-step of 0.4 μm, giving a 3-D volume of 20.8 μm^3 and 19.6 μm^3 respectively. From the stacks, extended focus projections (A, D) and surface-shaded projections (B, C, E, F) were produced. The extended focus projections (A, D) express the information with a pseudocolour scale (range white-red-yellow-green-blue-black) indicating the strength of the fluorescence intensity, where white is the strongest. The surface-shaded projections are visualized with yellow pseudocolour viewed at 0° latitude, 0° longitude (B, E) and rotated 180° longitude (C, F). Stratum corneum is located at the top in all photos. Size bar = 10 μm.

Table I. *Quantification of CD1a expression in epidermis with CLSM*[a]

Group	Individual	Relative volume of CD1a reactivity (%)				
		Non-occluded skin	True test®	Finn chamber®	Finn chamber® with water	Finn chamber® with petrolatum
1 (0 h)	1	16	21	14	14	15
	2	16	11	24	32	22
	3	23	38	32	42	58
2 (24 h)	1	22	16	19	22	16
	2	21	17	21	18	22
	3	23	24	17	24	27
3 (48 h)	1	14	55	20	21	30
	2	28	24	30	20	22
	3	25	53	43	42	35

[a]Cryostat sections, 25 μm thick, of the skin biopsy specimens were stained for CD1a with indirect immunofluorescence. The relative areas (%) of pixels with intensity values above a threshold 40 on an arbitrary intensity scale (range 0–255) in user-defined maps of the epidermis excluding stratum corneum are indicated. Five optical sections at 4 different fields of view giving a total of 20 optical sections per biopsy were scanned at ×400. Results are expressed as mean per biopsy, $n = 20$ optical sections. The time of taking skin biopsy specimens after occlusion for 48 h are given within parenthesis.

be less than 5% (typically about 2–3%). The density was then calculated by point-counting. In each stack, the relative area of pix_1 in each binary picture was determined by dividing the number of pix_1 in the user-defined map by the total number of pixels in the user-defined map. An average density was calculated for each stack (mean of five binary pictures) and skin biopsy (mean of twenty binary pictures, i.e. four stacks). Twenty sections per biopsy showed a variation of less than 10% from the progressive mean.

The laser power (7.0 mW) and the photomultiplier (PM)voltage (840 V) were calibrated in such way that the whole intensity scale was used. An ×40 plano-apochromate Nikon objective was used. Pixel size was 0.5 μm × 0.5 μm and the picture size was 512 × 512 pixels.

3-D reconstructions of LC

The distribution of dendrites of the LC in epidermis after the occlusion was examined by 3-D reconstructions. The laser power (varying from 7.0–11.0 mW) and PM voltage (870–910 V) were calibrated so that the whole intensity scale was used for each biopsy specimen. A ×100 plano-apochromate Nikon objective with oil-immersion was used. The pixel size was 0.2 μm × 0.2 μm and the picture size was 512 × 512 pixels. A typical 3-D reconstruction consisted of about fifty optical sections scanned with a z-increment of 0.4 μm. From each optical stack, extended focus projections (Fig. 2A, D) and surface-shaded projections (Fig. 2B, E and 2C, F) were calculated by the software provided by the SARASTRO® 2000 CLSM system. The surface-shaded projections were calculated from two different angles (0° latitude, 0° longitude and 0° latitude, 180° longitude), thus enhancing the visualization of the 3-D configuration of the object (Fig. 2B, E and 2C, F). In addition, the software allows calculation of projections from any (0–360°) desired angle. Each section in the optical stack was smooth-filtered twice and the threshold for signal-to-noise separation was obtained by the algorithm (19) described above.

Immunoperoxidase staining

Acetone-fixed vertical cryostat sections, 6 μm thick, were stained with the peroxidase-antiperoxidase method (20). Endogenous peroxidase was blocked by incubation in 0.3% H_2O_2 in PBS for 15 min. Normal rabbit serum (diluted 1/10) was then applied to the sections for 10 min to reduce non-specific staining. The mouse MoAb used were Leu-6 diluted 1/20, Leu-4 (IgG_{1k}, CD3, main cellular reactivity pan T cells) diluted 1/256, both from Becton Dickinson, and anti-ICAM-1 (84H10, IgG_1) diluted 1/80, from Serotec, Oxford, UK. Rabbit anti-mouse immunoglobulin (diluted 1/40), used as a secondary antibody, and pre-formed complexes of horseradish peroxidase and mouse monoclonal anti-horseradish peroxidase were obtained from Dakopatts. The peroxidase reaction was developed with 3-amino-9-ethylcarbazole (21) and the sections were counterstained with Mayers' haematoxylin. The dilutions of antibodies were determined using sections from normal lymph nodes and skin. Controls without the primary antibody or with irrelevant mouse MoAb gave no staining.

Light microscopy evaluation

The immunoperoxidase-stained sections were examined under coded conditions by one investigator (AE). At least two sections were included for each antibody and biopsy. The sections were viewed at ×400 using a standard eye-piece. Only the interfollicular part of epidermis was evaluated. The CD1a+ cells were counted in 7–15 fields of view per biopsy. Stained cells with at least one dendrite and a detectable cell nucleus were considered positive. The CD3+ cells were counted in 6–11 fields of view. The result of CD1a+ and CD3+ cell counting was calculated as the number of positive cells per field of view. The amount of ICAM-1 positivity in epidermis per biopsy was estimated on a semi-quantitative scale from 0 to 3 (0 = no, 1 = few, 2 = moderate, and 3 = many cells). The scale was adjusted so that 3 referred to the maximal number of positive cells within all specimens.

Statistical analysis

Friedman's non-parametric two-way analysis of variance (ANOVA) was used to evaluate the results. $p < 0.05$ was considered to be statistically significant.

RESULTS

Clinical assessment

The 9 persons in the three groups had no clinical signs of skin irritation at the time of taking punch biopsies.

Quantification of CD1a expression in epidermis with CLSM

The relative volume of CD1a reactivity varied between 14% and 28% in the biopsies from non-occluded skin and between 11% and 55% in the biopsies from occluded skin (Table I). No statistically significant differences were found between biopsies from non-occluded ($n = 9$) and occluded ($n = 36$) skin.

Table II. *Light microscopic enumeration of CD1a$^+$ cells in epidermis*[a]

Group	Individual	Number of CD1a$^+$ cells/field of view				
		Non-occluded skin	True test®	Finn chamber®	Finn chamber® with water	Finn chamber® with petrolatum
1 (0 h)	1	4.7	4.7	6.2	6.1	7.3
	2	4.9	6.3	6.4	8.7	6.5
	3	8.3	5.4	6.3	11	12.9
2 (24 h)	1	4.3	4.5	6.3	5.8	5.8
	2	6.1	4.9	6.9	8.1	7.7
	3	12.6	9	10	10	10.1
3 (48 h)	1	8.9	10.9	11.2	10.1	8
	2	8.2	10.3	9.6	11.2	6.4
	3	9	12.7	11.7	13.3	10.6

[a]Cryostat sections, 6 μm thick, of the skin biopsy specimens were stained for CD1a with immunoperoxidase. The CD1a$^+$ epidermal cells were counted in 7–15 fields of view at ×400 per biopsy. Stained cells with at least one dendrite and a detectable cell nucleus were considered positive. Results are expressed as number of CD1a$^+$ cells per field of view. The time of taking skin biopsy specimens after occlusion for 48 h are given within parenthesis.

Nor were any statistically significant changes detected when each group was analysed separately between biopsies from non-occluded ($n = 3$) and occluded ($n = 12$) skin.

3-D analysis of LC

All biopsies from the individuals in group 3 ($n = 15$) and those five from individual no. 3 in group 2 were processed for 3-D analysis of LC. The 3-D reconstructions of LC are exemplified from individual no. 3 in group 2, showing a non-specific projection of dendrites in normal skin. In skin occluded for 48 h with Finn chamber® and water and biopsied 24 h later, this was replaced by a pronounced projection of dendrites towards the skin surface (Fig. 2). The surface-shaded projections of normal and occluded skin were calculated from two different angles (Fig. 2B, C, E, F). The other biopsy specimens from occluded skin showed no detectable changes in the dendritic projections of the LC, or any other significant morphological changes compared to LC in non-occluded skin.

Immunoperoxidase analysis

CD1a expression. The inter-individual variation in the number of epidermal LC in non-occluded skin was 4.3–12.6 CD1a+ cells/field of view and in occluded skin 4.5–13.3 (Table II). There were no statistically significant changes in the number of CD1a+ cells when the three groups were analysed together between biopsies from non-occluded ($n = 9$) and occluded ($n = 36$) skin. Nor were any statistically significant differences detected when each group was analysed separately between biopsies from non-occluded ($n = 3$) and occluded ($n = 12$) skin.

CD3 expression. In non-occluded skin, CD3+ cells were found in the epidermis in individual no. 3 of group 1 (0.1 CD3+/ fields of view), in individual no. 3 of group 2 (0.3) and in individual no. 2 of group 3 (0.6). Directly after removal of the patch tests a slight increase of CD3+ cells in the epidermis was observed for all types of occlusion (Fig. 3A). The increase in the CD3+ cells was also found at 24 h and 48 h after occlusion in most biopsies (Fig. 3A). The CD3+ cells were mainly located in the basal part of the epidermis in all groups.

ICAM-1 expression. In non-occluded skin, expression of ICAM-1 was detected on a few keratinocytes in individual no. 2 in group 1 and individual no. 1 in group 3. The ICAM-1 expression on keratinocytes was greater for all types of occlusion at the time of removing the patch tests (Fig. 3B). Twenty-four hours later, the increase of ICAM-1 expression was less pronounced, except for occlusion with empty Finn chamber®. A slight increase compared to non-occluded skin was still found 48 h after the removal of patch tests (Fig. 3B). ICAM-1 was mainly expressed focally on keratinocytes in the basal part of the epidermis in all groups.

DISCUSSION

CLSM has proved to provide quantitative data on specific cellular populations and components in various tissues (16, 19). In addition, CLSM makes it possible to perform 3-D reconstructions of cells in the same tissue volume, thus allowing detailed morphological analysis. In the present study we used CLSM for quantitation and morphological analysis of the LC population in normal and occluded skin.

We found that there were no statistically significant differences in the relative volume of epidermal CD1a reactivity between the data from occluded skin and non-occluded skin. We also performed ordinary immunoperoxidase staining of the biopsy specimens and counted the number of CD1a+ epidermal cells. The inter-subject variation in the number of LC in epidermis in non-occluded skin was 4.3–12.6 per field of view, which is of the same magnitude as previously reported (9, 22). The number of LC in epidermis is known to vary widely between individuals and between different areas of the body, which is why the best control when investigating LC numbers in reactive skin is an individual's own adjacent normal skin

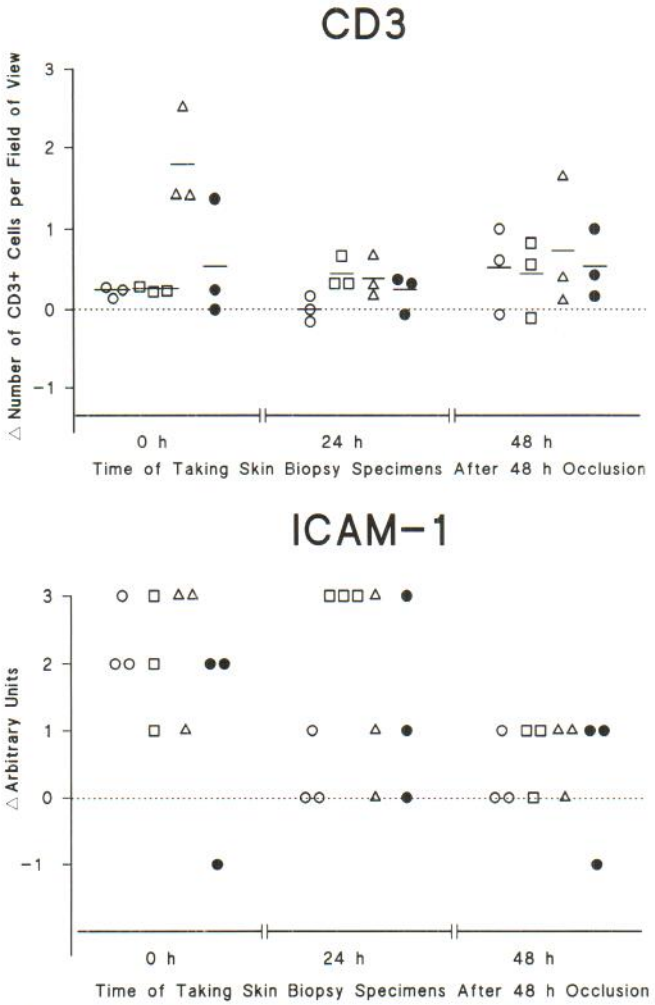

Fig. 3. Light microscopic evaluation of immunoperoxidase-stained, 6 μm thick cryosections of skin biopsies. The biopsies were taken after 48 h occlusion with True test® (○), empty Finn chamber® (□), Finn chamber® with water (△) and Finn chamber® with petrolatum (●) at 0 h, 24 h and 48 h after the occlusion. A) The CD3+ cells were counted in 6–11 fields of view per biopsy at ×400. The result for each biopsy was calculated from the difference between the number of CD3+ cells per field of view at ×400 in the biopsy and the result from the control non-occluded skin for each individual. Mean ($n = 3$) for each type of occlusion and time period is indicated with a horizontal bar. B) The ICAM-1 reactivity is expressed using a a semi-quantitative scale from 0 to 3 (0 = no, 1 = few, 2 = moderate, and 3 = many cells). The result for each biopsy specimen from each individual is given as the difference compared to non-occluded skin for each individual.

(22, 23). The result with immunoperoxidase was similar to that with CLSM, i.e. no statistically significant differences between non-occluded and occluded skin were found in the numbers of epidermal CD1a+ cells. Our result is in agreement with previous data to the effect that occlusion does not influence the number of epidermal LC (9) but conflicts with other reports (7, 8). These studies were also performed with immunoperoxidase on vertical skin sections (7–9). Apart from some differences in the experimental models used and the individual variations in susceptibility to occlusion, the difficulties of enumerating LC in vertical sections (10) may explain the diverging results.

In agreement with a previous report on different methods for enumerating LC (10), we believe that the best way to obtain information on changes in cell populations is to use stereological methods. Compared to ordinary light microscopy (10) there are several advantages with CLSM when using stereological methods on vertical sections: increased contrast as well as increased resolution, and the possibility to do optical sectioning of thick sections which allows exact evaluation of 3-D objects.

A new dimension of information is obtained when examining the 3-D projections. The possibility to visualize structural changes in a cell population is demonstrated by the reconstructions of LC in this study. The 3-D reconstructions and quantification of a specific cellular structure in a given tissue volume may enhance the interpretation of the link between structure and function. The pronounced projection of the LC dendrites towards the skin surface observed after occlusion with Finn chamber® with water (Fig. 2) suggests an LC reaction to the change induced in the environment.

The present study shows that even a mild external stimulus such as occlusion with patch tests (either True test® or Finn chamber®) produces a transient mild inflammatory reaction with an induced expression of ICAM-1 on keratinocytes and an increased number of CD3+ epidermal lymphocytes as determined with immunoperoxidase staining. Our results agree with a previous report (24) that the occurrence of CD3+ cells in the skin under inflammatory conditions is associated with the expression of ICAM-1 in the epidermis.

In conclusion, the present study demonstrates that occlusion induces a transient response in the skin compatible with an inflammatory reaction. No significant changes were found in either the number of LC or in the relative volume of LC between normal and occluded skin. In addition, we have demonstrated that CLSM can offer 3-D information on morphological changes in the LC. This new technique should thus provide data for a deeper understanding of pathophysiological mechanisms in the skin.

ACKNOWLEDGEMENTS

This study was supported by grants from the Swedish Work Environment Fund, the Swedish Medical Research Council (project 16X-7294), the King Gustav V Foundation, the Swedish Association against Asthma and Allergy, the Finsen Foundation, the Edvard Welander Foundation and the Hesselman Foundation. We thank Mrs Anne Svensson for excellent technical assistance, PhD Kjell Carlsson, the Royal Institute of Technology, Stockholm, for constructive criticism and valuable help on the ISIS system, and MSc Ulf Brodin, the Department of Medical Information Processing, Karolinska Institute, Stockholm, for valuable help with the statistics.

REFERENCES

1. Berardesca E, Maibach HI. Skin occlusion: treatment or drug-like device? Skin Pharmacol 1988; 1: 207–215.
2. Fisher LB, Maibach HI, Trancik RJ. Effects of occlusive tape systems on the mitotic activity of epidermis. With and without corticosteroids. Arch Dermatol 1978; 114: 384–386.
3. Hinman CD, Maibach HI. Effect of air exposure and occlusion on experimental human skin wounds. Nature 1963; 200: 377–378.

4. Alvarez OM, Mertz PM, Eaglstein WH. The effect of occlusive dressings on collagen synthesis and re-epithelialization in superficial wounds. J Surg Res 1983; 35: 142–148.
5. Lindberg M, Johannesson A, Forslind B. The effect of occlusive treatment on human skin: an electron microscopic study on epidermal morphology as affected by occlusion and dansyl chloride. Acta Derm Venereol (Stockh) 1982; 62: 1–5.
6. Lindberg M, Forslind B. The effects of occlusion of the skin on the Langerhans' cell and the epidermal mononuclear cells. Acta Derm Venereol (Stockh) 1981; 61: 201–205.
7. Mikulowska A. Reactive changes in the Langerhans' cells of human skin caused by occlusion with water and sodium lauryl sulphate. Acta Derm Venereol (Stockh) 1990; 70: 468–473.
8. Lindberg M, Emtestam L. Dynamic changes in the epidermal OKT6 positive cells at mild irritant reactions in human skin. Acta Derm Venereol (Stockh) 1986; 66: 117–120.
9. Nieboer C, Bruynzeel DP, Boorsma DM. The effect of occlusion of the skin with transdermal therapeutic system on Langerhans' cells and the induction of skin irritation. Arch Dermatol 1987; 123: 1499–1502.
10. Bieber T, Ring J, Braun-Falco O. Comparison of different methods for enumeration of Langerhans cells in vertical cryosections of human skin. Br J Dermatol 1988; 118: 385–392.
11. Cox IJ, Sheppard CJR, Wilson T. Super-resolution by confocal fluorescent microscopy. Optik 1982; 60: 391–396.
12. Carlsson K, Åslund N. Confocal imaging for 3-D digital microscopy. Appl Opt 1987; 26: 3232–3238.
13. Wilson T, ed. Confocal microscopy. London: Academic Press, 1990.
14. Scheynius A, Lundahl P. Three-dimensional visualization of human Langerhans' cells using confocal scanning laser microscopy. Arch Dermatol Res 1990; 281: 521–525.
15. Carlsson K, Wallén P, Brodin L. Three-dimensional imaging of neurons by confocal fluorescence microscopy. J Microscopy 1989; 155: 15–26.
16. Scheynius A, Dalenbring M, Carlsson K, England R, Lindberg M. Quantitative analysis of Langerhans' cells in epidermis at irritant contact reactions using confocal laser scanning microscopy. Acta Derm Venereol (Stockh) 1992; 72: 348–351.
17. Johnson GD, Davidson RS, McNamee KC, Russell G, Goodwin D, Holborow EJ. Fading of immunofluorescence during microscopy: a study of the phenomenon and its remedy. J Immunol Methods 1982; 55: 231–242.
18. Pawley JB, ed. Handbook of biological confocal microscopy. New York: Plenum Press, 1990.
19. Mossberg K, Arvidsson U, Ulfhake B. Computerized quantification of immunofluorescence-labeled axon terminals and analysis of co-localization of neurochemicals in axon terminals with a confocal scanning laser microscope. J Histochem Cytochem 1990; 38: 179–190.
20. Sternberger LA. Immunohistochemistry. New York: Wiley Medical Publications, John Wiley & Sons, Inc., 1979.
21. Kaplow LS. Substitute for benzidine in myeoloperoxidase stains. Am J Clin Pathol 1975; 63: 451.
22. Ashworth J, Turbitt ML, Mackie R. The distribution and quantification of the Langerhans cell in normal human epidermis. Clin Exp Dermatol 1986; 11: 153–158.
23. Horton JJ, Allen MH, MacDonald DM. An assessment of Langerhans cell quantification in tissue sections. J Am Acad Dermatol 1984; 11: 591–593.
24. Singer KH, Tuck DT, Sampson HA, Hall RP. Epidermal keratinocytes express the adhesion molecule intercellular adhesion molecule-1 in inflammatory dermatoses. J Invest Dermatol 1989; 92: 746–750.